AIAA JOURNAL
Vol. 39, No. 8, August 2001

Technical Notes

TECHNICAL NOTES are short manuscripts describing new developments or important results of a preliminary nature. These Notes cannot exceed six manuscript pages and three figures; a page of text may be substituted for a figure and vice versa. After informal review by the editors, they may be published within a few months of the date of receipt. Style requirements are the same as for regular contributions (see inside back cover).

Geometry-Based Hyperbolic Grid Generation for Computational Fluid Dynamics

S. Anil Lal,* B. V. S. S. S. Prasad,† and N. Sitaram‡
Indian Institute of Technology, Madras, Chennai 600 036, India

Introduction

In computational fluid dynamics hyperbolic grid system is best suited for obtaining orthogonal grids near solid walls for accurately estimating the fluxes and gradients of flow properties. The available hyperbolic grid-generation techniques are based on two coupled nonlinear, hyperbolic partial differential equations: one for the cell area (Jacobian) and the other for the orthogonality.[1] These equations typically require a linearization procedure and a block tridiagonal matrix solver for their numerical solution.[2] In some cases artificial dissipation terms are added for dampening the grid oscillations.[3] Such numerical methods, though mathematically elegant, are complex and time consuming. In this Note simple algebraic relations based on analytical geometry are derived for ensuring the orthogonality and providing required cell area.

Methodology

The boundary curve chosen for grid generation is defined by a set of discrete data points. The grid generation is carried out by starting from the boundary curve and marching in successive layers. The boundary curve is regarded as the base curve for the generation of the first grid layer. Quadrilateral cells are constructed on outward normals at all grid points of the base curve. The outer surface of these cells is treated as the base curve for the generation of the next grid layer. This marching process is continued until a prescribed number of (say, N) layers are formed. The procedure for obtaining the outward normals and the cell area is explained in the following sections.

Construction of Outward Normal

Consider a base curve Γ_i in Fig. 1, which has discretized points such as a, b, and c. At point b, bm, and bn are unit vectors along the outward normals of the edges ab and bc, respectively. The outward normal at the point b of the curve Γ_i is along the ray bo, which is the bisector of angle $\angle mbn$. The coordinates of the points m, n, and o are derived as

$$(x_m, y_m) = \left[\left(x_b l^i_{ab} - y_b + y_a\right)\Big/ l^i_{ab}, \left(y_b l^i_{ab} + x_b - x_a\right)\Big/ l^i_{ab}\right] \quad (1)$$

$$(x_n, y_n) = \left[\left(x_b l^i_{bc} + y_b - y_c\right)\Big/ l^i_{bc}, \left(y_b l^i_{bc} - x_b + x_c\right)\Big/ l^i_{bc}\right] \quad (2)$$

$$(x_o, y_o) = [(x_m + x_n)/2, (y_m + y_n)/2] \quad (3)$$

where l^i_{ab} and l^i_{bc} are lengths of the edges ab and bc on Γ_i, respectively.

Cell Area

Consider that a cell should be constructed about an edge ab. The cell area is a function of the length of the specific edge l^i_{ab} on the base curve Γ_i, length of the corresponding edge l^1_{ab} on the boundary curve (Γ_1), and a distance parameter δ_i, $i = 1$ to N. The distance parameter δ determines the normal dimension of the cell. It is formulated with the help of an exponential stretching function:

$$\frac{\delta_i}{\Delta} = 1 - \left[\frac{\exp[s(N-i)/(N-1)] - 1}{e^s - 1}\right] \quad (4)$$

where $\Delta = \delta_N$, the value of Δ is chosen as a function of the characteristic dimension in question, e.g., chord length C_h for an airfoil.

The area of cell formed over the edge ab on Γ_i is obtained by giving chosen weightages to the lengths of edges on the boundary curve Γ_1 and the base curve Γ_i. This area A_{abed} is given by

$$A_{abed} = \left[l^i_{ab}\varepsilon + l^1_{ab}(1-\varepsilon)\right]h_i \quad (5)$$

where ε is called the cell size control factor and $h_i (= \delta_i - \delta_{i-1})$ is the cell height. A suitable value for ε (between 0 and 1) is selected to get an appropriate cell size distribution within the domain.

Cell Construction

The cell above the edge ab of Fig. 1 is formed by knowing the coordinates of the points a, b, d, o and the prescribed cell area A_{abed}. Here e is the grid point in the new layer, and it corresponds to the point b on the base curve. Whereas the coordinates of the point o are calculated from Eqs. (1–3), the coordinates of point d are obtained during the cell formation on the preceding edge of ab. From the

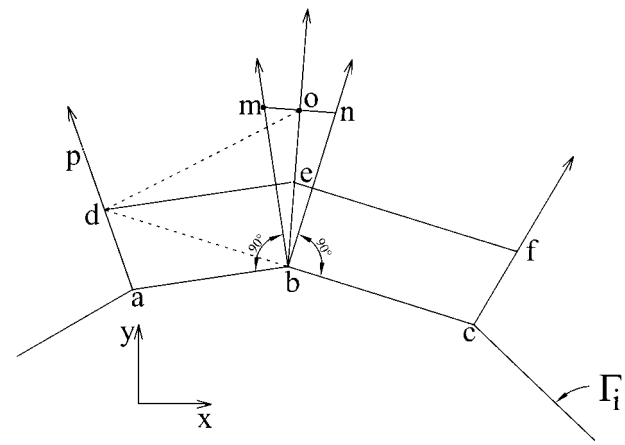

Fig. 1 Schematic diagram illustrating the hyperbolic grid-generation method.

Received 28 November 2000; revision received 20 March 2001; accepted for publication 4 April 2001.

*Research Scholar, Thermal Turbomachines Laboratory, Department of Mechanical Engineering.
†Professor, Department of Mechanical Engineering, Thermal Turbomachines Laboratory; prasad@acer.iitm.ernet.in.
‡Associate Professor, Thermal Turbomachines Laboratory, Department of Mechanical Engineering.

properties of triangles *dbe* and *dbo* in Fig. 1, the ratio of areas A_{dbe} and A_{dbo} is equal to the ratio of the lengths l_{be} and l_{bo}. Thus, the coordinates of the point e are estimated as

$$(x_e, y_e) = [f x_o + (1 - f)x_b,\ f y_o + (1 - f)y_b] \tag{6}$$

where

$$f = l_{be}/l_{bo} = A_{dbe}/A_{dbo} = (A_{abed} - A_{abd})/A_{bod}$$

The initial cells of every layer are constructed as rectangular cells.

Method of Damping Grid Oscillations

Dampening grid oscillations in the present method is done by averaging the normal distances. For instance, the point e in Fig. 1 is relocated to e', such that the distance between b and e' is the arithmetic mean of the distances l_{ad}, l_{be}, and l_{cf}. In this manner all of the points in the new grid layer are relocated repeatedly for a few iterations, typically five times. For situations such as sharp corners where there is a danger of grid line intersection, the cell height (h_i) in Eq. (5) is varied linearly to facilitate gradual turning of grid lines. Thus while smoothing the grid, small variations in cell area are allowed.

Results and Discussion

Figure 2a shows the hyperbolic grid generated over an ellipse having a major axis of 2 units and a minor axis of 0.2 units with $\Delta = 1$, $N = 20$, $s = -5$, and $\varepsilon = 0.25$. Figure 2b shows the enlarged view of the grid near the trailing edge when ε takes a value of unity. As ε increases, the grid lines near the rear stagnation point tend to diverge as the cell areas increase from inner layers to the outer. Figure 3 shows the grid generated around a 90-deg sharp corner with $\Delta = 1$, $N = 20$, $s = -1$, and $\varepsilon = 0.5$, which demonstrates the capability of the method to discretize open geometries having sharp corners. The case of possible grid line intersection is handled with controlled cell area variations for the corner (cavity) problem, shown in Fig. 4.

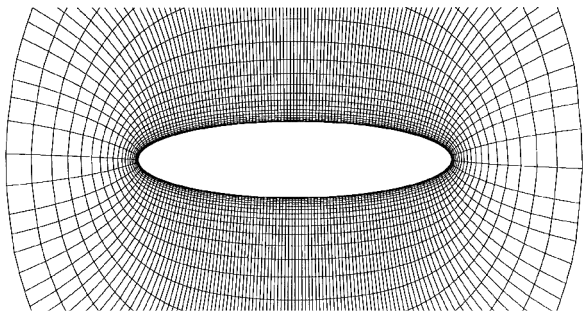

a) $\varepsilon = 0.25$

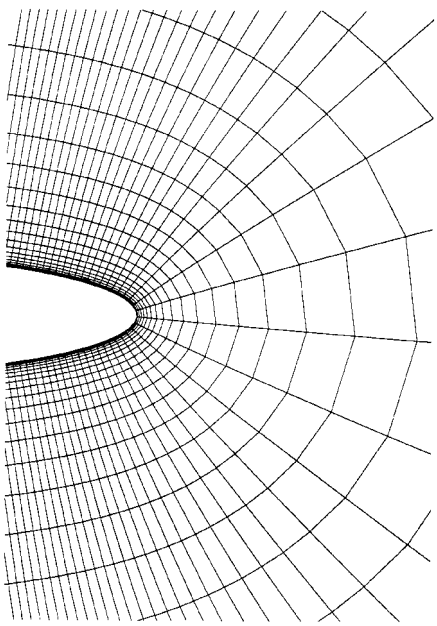

b) $\varepsilon = 1$

Fig. 2 Hyperbolic grid generated around an ellipse with grid smoothing ($\Delta = 1$, $N = 20$, $s = -5$).

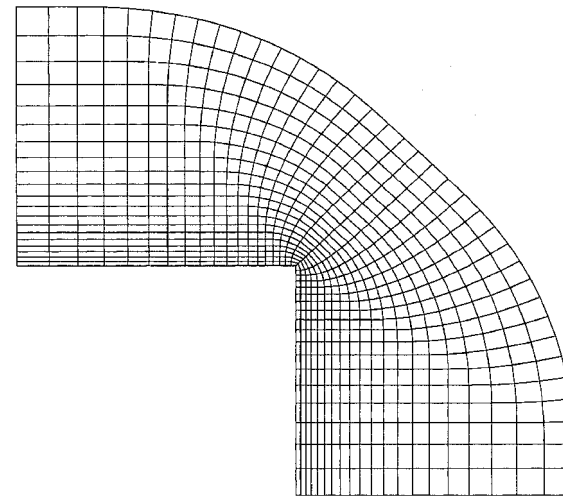

Fig. 3 Grid exterior to a corner.

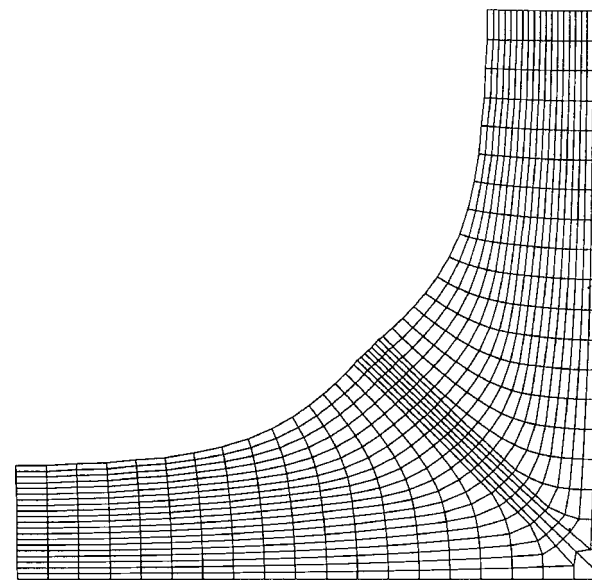

Fig. 4 Grid inside the corner of a cavity.

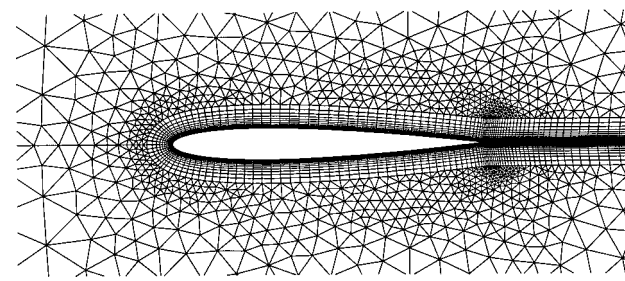

Fig. 5 Hybrid grid system around NACA-0012 airfoil.

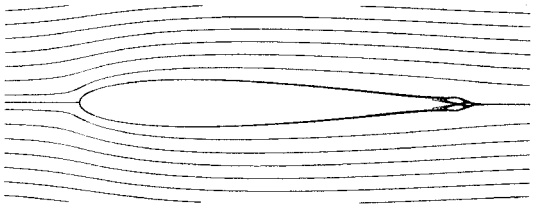

a) Streamline plot in laminar flow

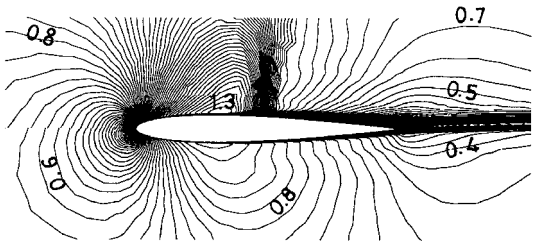

b) Mach contours in turbulent flow

Fig. 6 Flow over an isolated NACA-0012 airfoil.

A C-type boundary-layer grid around a NACA-0012 airfoil has been generated up to a normal distance corresponding to $\Delta/C_h = 0.06$. The values of N and s are 20 and -4, respectively. This boundary-layer mesh is coupled and with unstructured and algebraic meshes as shown in Fig. 5. Figure 6a shows the streamlines in laminar flow with the conditions for freestream Mach number $M_\infty = 0.5$, Reynolds number based on chord $Re_{ch} = 5 \times 10^3$ and incidence $\alpha = 0$ deg, same as those used by Liu.[4] The present results, including a small separation zone near the trailing edge, are in good agreement with Liu.[4] Figure 6b shows the isentropic Mach-number contours for the turbulent compressible flow at $M_\infty = 0.754$, $Re_{ch} = 3.76 \times 10^6$, and $\alpha = 3.02$ deg. With the help of hyperbolic grid, the Baldwin–Lomax turbulence model has been implemented without any complex changes, such as those suggested by Turner and Jennions.[5] The standard k–ε model is used in the unstructured and algebraic grid zones. This result is in good agreement with the predictions of Kallinderis.[6]

Conclusions

A hyperbolic grid-generation technique is proposed based on analytical geometric considerations. The main feature of the method is generation of orthogonal quadrilateral cells with controllable cell area. The grid generated by the proposed method is found to be convenient for accurate prediction of laminar and turbulent flow past arbitrary shaped bodies.

References

[1]Thompson, J. F., "Grid Generation Techniques in Computational Fluid Dynamics," *AIAA Journal*, Vol. 22, No. 11, 1984, pp. 1505–1523.

[2]Hoffman, K. A., and Chiang, S. T., "Grid Generation-Structured Grids," *Computational Fluid Dynamics for Engineers*, Vol. 1, Engineering Education Systems, Wichita, KS, 1993, pp. 344–411.

[3]Tai, C. H., Yin, S. L., and Sorg, C. Y., "A Novel Hyperbolic Grid Generation Procedure with Inherent Adaptive Dissipation," *Journal of Computational Physics*, Vol. 116, No. 1, 1995, pp. 173–179.

[4]Liu, F., "Numerical Calculation of Turbomachinery Cascade Flows," Ph.D. Dissertation, Dept. of Mechanical and Aerospace Engineering, Princeton Univ., Princeton, NJ, June 1991.

[5]Turner, M. G., and Jennions, I. K., "An Investigation of Turbulence Modelling in Transonic Fans Including a Novel Implementation of an Implicit k–ε Turbulence Model," *Journal of Turbomachinery*, Vol. 115, No. 2, 1993, pp. 249–307.

[6]Kallinderis, Y., "Algebraic Turbulence Modelling for Adaptive Unstructured Grids," *AIAA Journal*, Vol. 30, No. 3, 1992, pp. 631–639.

J. Kallinderis
Associate Editor

Mixing Enhancement in Compressible Base Flows via Generation of Streamwise Vorticity

C. J. Bourdon* and J. C. Dutton†
University of Illinois at Urbana–Champaign, Urbana, Illinois 61801

Introduction

PREVIOUS studies employing flow visualization techniques and pitot pressure measurements[1–3] have shown that asymmetries in the pressure field of the jets issuing from ideally expanded converging and ideally or overexpanded converging–diverging nozzles are caused by stationary streamwise vortices present in the flowfield. The origins of these vortices have been traced to imperfections in the nozzle surface. Krothapalli et al.[3] assert that imperfections as small as $\frac{1}{12}$th of the boundary-layer velocity deficit thickness are sufficient to trigger such behavior.

Stationary streamwise vortices such as these were shown to improve the mixing characteristics of axisymmetric jet flows[4] by increasing the stream interface area and overall shear layer thickness. Therefore, these researchers found it beneficial to promote streamwise vorticity generation by inserting surface disturbances onto the nozzle lip. King et al.[4] found that the most effective shape for generating streamwise vortices in a supersonic jet is an isosceles triangular tab, placed flush on the surface, with an apex angle of 25–30 deg. This study also found that increasing the tab thickness increased the shear layer thickness, although the benefit was relatively small when compared to that of the thinnest significant tab disturbance.

Extension of such a technique to base flows seems quite natural. If the streamwise vorticity generated from the tabs survives the base corner expansion fan, which has been shown[5] to damp turbulence in the developing shear layer, it could significantly influence the turbulence structural organization in the near-wake region. Influencing the turbulent structure organization (and thus mixing between the freestream and core fluid) may substantially alter the base pressure and drag characteristics of a bluff object. This is the subject of the current Note.

Flow Facility and Equipment

The axisymmetric, supersonic flow facility in the University of Illinois Gas Dynamics Laboratory was employed in this study. The base model is supported by a 63.5-mm-diam sting, which extends through the supersonic converging–diverging nozzle. The freestream flow before separation from the base model is at a Mach number of 2.46, with a unit Reynolds number of 52×10^6 m^{-1}, and typical stagnation conditions of $P_0 = 368$ kPa and $T_0 = 300$ K. The turbulent boundary-layer thickness on the sting/afterbody just before separation has been measured to be 3.2 mm (Ref. 5). A schematic of the main features of the base region are given in Fig. 1.

The surface disturbances were formed in this study by application of pieces of adhesive shipping label to the surface of a blunt-based afterbody. As stated earlier, disturbances as small as $\frac{1}{12}$th of the velocity deficit thickness have been found sufficient to produce asymmetries in overexpanded and ideally expanded jets.[3] In our facility, this translates to a disturbance thickness of approximately 0.1 mm (Ref. 5), the approximate thickness of the shipping label material. The disturbance thickness was altered by applying multiple layers of the labeling material.

Received 11 March 2001; revision received 16 April 2001; accepted for publication 18 April 2001.

*Graduate Research Assistant, Department of Mechanical and Industrial Engineering. Student Member AIAA.

†W. Grafton and Lillian B. Wilkins Professor, Department of Mechanical and Industrial Engineering. Associate Fellow AIAA.